

Dynamics of the “Strong” Polymer of *n*-Lauryl Methacrylate below and above the Glass Transition

G. Floudas,^{*,†} P. Placke,[‡] P. Štěpánek,[§] W. Brown,^{||} G. Fytas,[†] and K. L. Ngai[⊥]

Foundation for Research and Technology–HELLAS (FORTH)–Institute of Electronic Structure and Laser, P.O. Box 1527, 71110 Heraklion, Crete, Greece, Max-Planck-Institut für Polymerforschung, Postfach 3148, D-55021 Mainz, Germany, Institute of Macromolecular Chemistry, Academy of Sciences of the Czech Republic, 16206 Prague, Czech Republic, Department of Physical Chemistry, University of Uppsala, Box 532, 75121 Uppsala, Sweden, and Naval Research Laboratory, Washington, D.C. 20375-5320

Received April 7, 1995; Revised Manuscript Received July 24, 1995*

ABSTRACT: Dielectric spectroscopy (DS) and dynamic light scattering (DLS) are employed to study the dynamics of poly(*n*-lauryl methacrylate) (PnLMA) ($M_w = 1.1 \times 10^6$) at temperatures below and above the glass transition temperature T_g ($T_g \approx 225$ K). The DS and DLS data show no evidence for the splitting between the primary (α -) and secondary (β -) relaxations within the experimental frequency range. The main process affecting DS and DLS is the mixed $\alpha\beta$ -relaxation which bears similarities to a single α -process with regard to the T -dependence of the relaxation times. Excellent agreement between the two sets of experimental relaxation times was found. The distribution of relaxation times exhibits a pronounced temperature dependence: from a Kohlrausch–Williams–Watts (KWW) exponent of $\beta_{KWW} \approx 0.25$ at $T \approx T_g$ to $\beta_{KWW} \approx 1$ at $T \approx T_g + 100$ K and at a frequency of about 1 MHz. PnLMA is therefore, to our knowledge, the only polymer with a Debye ($\beta = 1$) distribution of relaxation times at megahertz frequencies so far. The extremely broad distribution near T_g and the weak normalized temperature dependence of the relaxation time apparently contradict the phenomenologically established correlation between the two in many glass formers. This contradiction might arise from concentration fluctuations of the long alkyl chain which can broaden the relaxation spectrum near T_g . In addition to the main β -process, a “fast” β -relaxation can be resolved in both experiments and originates from the polyethylene-like alkyl chain.

Introduction

There is a long history in the study of the relaxation properties of the poly(*n*-alkyl methacrylates).¹ A recurring theme is in the systematic study of relaxation properties in a series of these polymers with increasing length of the alkyl group in the side chain. One purpose of these systematic studies is to find the trend of variation in relaxation properties with chemical structural change in this family of polymers. An early example of these works includes the dynamic mechanical measurements made by Ferry and co-workers² in the frequency range 20–3000 Hz. The polymers studied were poly(ethyl methacrylate) (PEMA), poly(*n*-butyl methacrylate) (PnBMA), poly(*n*-hexyl methacrylate) (PnHMA), poly(*n*-octyl methacrylate) (PnOMA), and poly(*n*-lauryl methacrylate) (PnLMA), which was called poly(*n*-dodecyl methacrylate) (PnDMA) by Ferry. Another is the measurement of the loss modulus G'' at 1 Hz as a function of temperature of poly(methyl methacrylate) (PMMA), PEMA, poly(*n*-propyl methacrylate) (PnPMA), and PnBMA by Heijboer.³ Heijboer's results show that, with increasing length of the alkyl group, the position of the α -relaxation peak moves to lower temperatures with the tendency to merge with the β -relaxation peak which appears to remain stationary. Therefore, depending on the length of the alkyl chain (l) one can shift the glass transition temperature (an effect known as internal plasticization) by more than 150 K in going from the first member of the series

PMMA to $l = 12$ (PnLMA). As a consequence, for different l , one can study (i) the primary (α -) relaxation, (ii) the secondary (β -) relaxation, and (iii) the splitting region and the mixed $\alpha\beta$ -relaxation. Using PnLMA we are practically studying the mixed relaxation above T_g and the low- T relaxations.

For the lower members of this series, there exist extensive dielectric¹ and recently light scattering studies. The primary and secondary relaxations in the dielectric (DS) and dynamic depolarized light scattering (DLS) experiments are associated with the ester side group which possess most of the dipole moment and optical anisotropy, respectively. The DS response of the lower members of the series PMMA,^{4,5} PEMA,^{4,5} and PnBMA⁵ is influenced by the segmental (α -) and secondary (β -) relaxations. For PnHMA,⁶ however, only a single process could be detected with a temperature-dependent distribution of relaxation times which narrows with increasing T but remains broader than a single Debye process. The reason behind the inability of separating the two processes is the progressive shift of the merging of the two relaxations to lower frequencies with increasing alkyl chain length. Application of pressure was very successful in separating the two processes in the higher members of the series with alkyl chain lengths $l = 8^5$ and $l = 9.^7$ However, application of pressure on PnLMA⁷ did not succeed in separating the two processes, and the single DS process was discussed in terms of a mixed $\alpha\beta$ -process.

Recently, dynamic light scattering with the use of the modern correlators encompassing a broad time range has been applied to separate the two processes in poly(*n*-alkyl methacrylates). This was successful in PMMA,⁸ PEMA,⁹ and PnBMA,^{10,11} but for PnHMA¹² again a single process has been detected. The effect of introducing a bulkier side group has also been studied in poly-

* FORTH–Institute of Electronic Structure and Laser.

† Max-Planck-Institut für Polymerforschung.

‡ Academy of Sciences of the Czech Republic.

§ University of Uppsala.

|| Naval Research Laboratory.

⊥ Abstract published in *Advance ACS Abstracts*, September 1, 1995.

(cyclohexyl methacrylate) (PcHMA)^{13–15} where the β -relaxation is considerably suppressed. External plastification¹⁶ of PMMA with the polar additive DOP resulted in the strengthening of the β -relaxation at the expense of the primary relaxation. This was discussed in terms of a concerted motion of the polymer side chain with the polar additive.¹⁶

The purpose of the present study is to explore in detail (i) the modification of segmental dynamics by the introduction of a long side chain at temperatures above T_g and (ii) the local dynamics below T_g . The system is PnLMA, and the techniques are DLS and DS. Because of the low-frequency merging of the α - and β -relaxations (which we call here the "slow" β -relaxation to differentiate from a faster β -process), we are practically studying the mixed ($\alpha\beta$) relaxation which bears many similarities to the segmental (α -) relaxation. The distribution of relaxation times associated with this process displays an unusually strong T -dependence. It starts out extremely broad at low temperatures near T_g , narrows monotonically with increasing temperature, and becomes practically a single exponential at a frequency of 1 MHz. PnLMA is therefore, to our knowledge, the only polymer showing a Debye distribution of relaxation times at MHz frequencies. On the other hand, the characteristic relaxation time of the distribution has a weak dependence on the normalized reciprocal temperature T_g/T . These two features of the relaxation spectrum at first sight seem to violate the expected correlation between them (i.e., a broader spectrum together with a strong temperature dependence of the relaxation time) which has been established in many glass formers including polymers.^{17–19} However, this apparent contradiction can be removed since the long side chain in PnLMA gives rise to concentration fluctuations. These contribute a temperature-dependent broadening of the relaxation spectrum as observed. The additional relaxations at low- T studied by DLS and DS originate from the polyethylene (PE)-like side chain.

Experimental Section

Sample. Lauryl methacrylate monomer (Aldrich Chemicals) was carefully dried and vacuum distilled into the dust-free light scattering ampoule. Thermal polymerization was accomplished by heating the ampoule, sealed under vacuum at 393 K for 36 h. The sample was allowed to remain in the oven for 1 month at 373 K to attain equilibrium. The weight-average molecular weight M_w was 1.1×10^5 as determined by gel permeation chromatography (GPC) calibrated with a PMMA standard, and the polydispersity index (M_w/M_n) was 1.9. The glass transition temperature T_g was determined by differential scanning calorimetry (DSC). The sample was first cooled to 123 K at a rate of 15 K/min, and a thermogram was taken as it was heated to 373 K at a rate of 20 K/min and a second thermogram was recorded after cooling to 123 K (rate: 15 K/min) and subsequent heating with a rate of 10 K/min. A broad transition range was found in the vicinity of ~ 225 K with a breadth $\Delta T_g = 30$ K exceeding the values of other poly(n -alkyl methacrylates) with shorter alkyl chains. A lower T_g value (~ 208 K) was reported earlier by dilatometry.²⁰ There was also evidence for a melting peak centered at about 240 K with a $\Delta T_m \sim 15$ K (see inset to Figure 1). The melting point of PnLMA has been reported²¹ to occur at 239 K in agreement with our DSC result, but the dilatometric data showed no evidence for it. However, it has been reported²² that a minimal length of 10 carbon atoms is required for side-chain crystallization.

To investigate further the possibility of side-chain crystallization, we have used X-ray diffraction. A Siemens θ - θ diffractometer (D500T) was used in the reflection geometry as described elsewhere.²³ Measurements were made in the

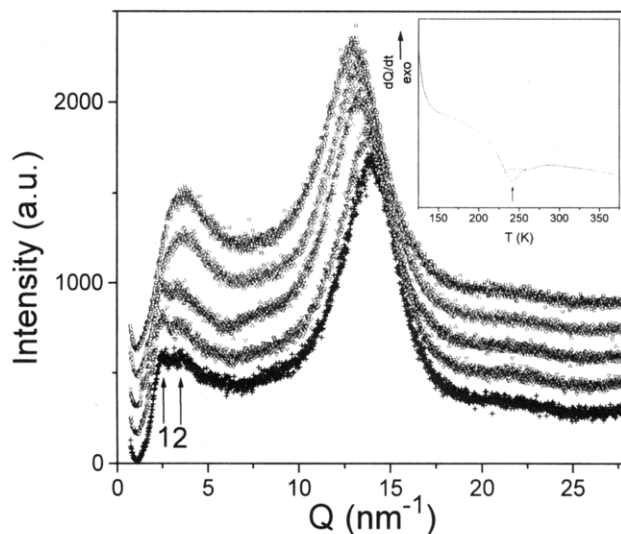


Figure 1. Wide-angle X-ray scattering curves for PLMA for different temperatures: (\square) 333, (\circ) 298, (\triangle) 243, (∇) 233, and ($+$) 223 K. The melting point of PnLMA is 239 K, and at this temperature there is evidence for weak crystallization (additional peaks 1 and 2). The melting point is also evident by DSC (arrow at the inset) together with a broad glass transition.

Q -range 1–28 nm^{−1} and for several temperatures between 223 and 333 K. Figure 1 shows the X-ray diffraction patterns at some temperatures. These patterns are characterized by a strong amorphous peak at $Q \approx 13$ nm^{−1}, corresponding to a distance of ~ 5 Å. This peak is considered to arise from the van der Waals (VDW) contacts of atoms and is referred to as the VDW peak. The temperature dependence of this peak has been studied earlier in two polycarbonates of Bisphenol A²³ and reflects the different thermal expansion below and above T_g . There is also an additional peak at lower Q , referred to as the low van der Waals (LVDW) peak, with a smaller intensity than the VDW peak which originates from structures with a spacing of $d \sim 18$ Å at $T = 298$ K. The diffraction patterns at the two lowest measurement temperatures (223 and 233 K) provide evidence for weak crystallization with corresponding spacings of 25 and 18 Å (arrows in Figure 1). The observed weak crystallization in PnLMA contrasts with the sharp diffraction peaks in poly(n -octadecyl methacrylate)²⁴ due to side-chain crystallization.

Dynamic Light Scattering (DLS). Samples of high optical quality are necessary for photon correlation spectroscopy (PCS) studies of bulk polymers near and below T_g . To check the optical quality of our sample, we have recorded a polarized (VV) Rayleigh–Brillouin (RB) spectrum at 294 K, using a tandem Fabry–Perot interferometer (FPI) with a free spectral range of 30 GHz. The RB spectrum is shown in Figure 2 and displays the central peak and the shifted Brillouin doublet. The Landau–Placzek (LP) intensity ratio, that is, the intensity ratio of the unshifted peak to the shifted Brillouin doublet, is 4.8, and the frequency shift f_B and width $2\Gamma_B$ of the Brillouin lines are 8.26 and 1.25 GHz, respectively. The low LP ratio is indicative of a sample with high optical quality which allows us to proceed to our PCS study. It is worth noticing the broad Brillouin linewidth at about $T_g + 70$ K, similar to other poly(n -alkyl methacrylates)⁶ with shorter alkyl side chains.

The depolarized (V_H) geometry was used for the PCS study, and the apparatus used was equipped with an argon ion laser (Coherent Radiation, Model Innova 300) operating at a wavelength of 488 nm. The incident and scattered beams were polarized, respectively, with Glan (extinction coefficient better than 10^{-6}) and Glan–Thompson (extinction coefficient better than 10^{-7}) polarizers. The detection optics employed a 4- μ m-diameter monomodal fiber coupled to the photomultiplier. The index-matching fluid was silicone oil, cooled using a cryostat. Condensation on the cell windows at subzero temperatures was prevented by a N₂ stream onto the exposed surfaces. An

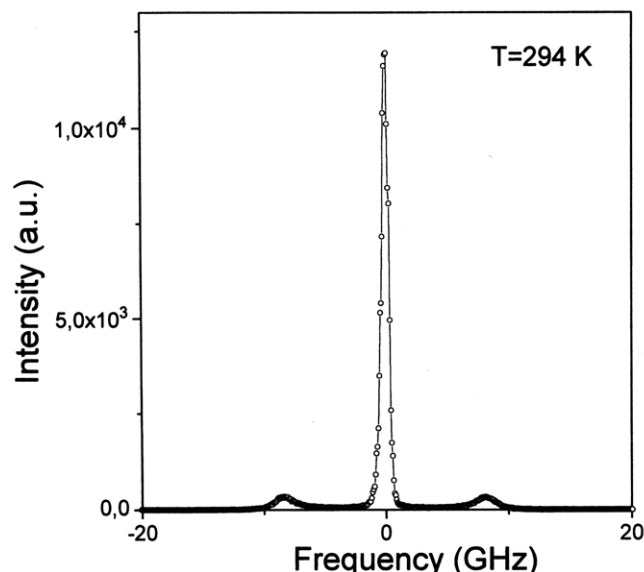


Figure 2. Polarized Rayleigh-Brillouin spectrum of PnLMA taken with FSR of 30 GHz at 294 K. At this temperature the Landau-Placzek intensity ratio is about 5.

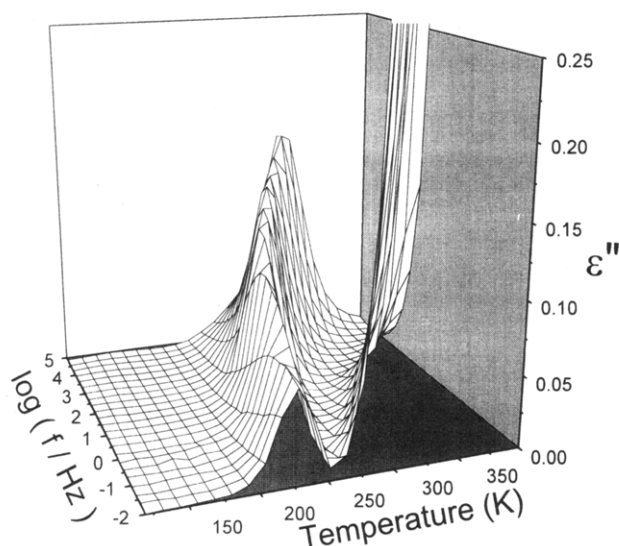


Figure 3. 3D representation of the dielectric loss ϵ'' as a function of temperature and frequency.

ALV-5000 multibit, multi- τ full digital autocorrelator was used. Details on the experimental setup can be found elsewhere.¹⁶

Dielectric Spectroscopy (DS). Measurements of the complex dielectric function were made in the frequency range from 10^{-2} to 10^5 Hz with a frequency response analyzer (Solartron Schlumberger FRA1260) and for temperatures between 123 and 315 K. The sample was kept between two gold-plated stainless steel plates of 20 mm diameter with a separation of 50 μm . The sample environment and details on the experimental setup are given in ref 25. Typical dielectric loss curves are shown in Figure 3, in a 3D representation.

Mechanical Spectroscopy (MS). Measurements of the complex shear modulus G^* were made with a Rheometrics RMS800 spectrometer over the temperature range from 183 to 343 K and for 10 frequencies between 0.1 and 100 rad/s. The temperature was controlled with an accuracy of ± 0.5 K, and the amplitude of deformation was within the linear viscoelastic range.

Data Analysis

Dynamic Light Scattering (DLS). On the basis of the relatively low Landau-Placzek intensity ratio and the weak depolarized scattered intensity, we have

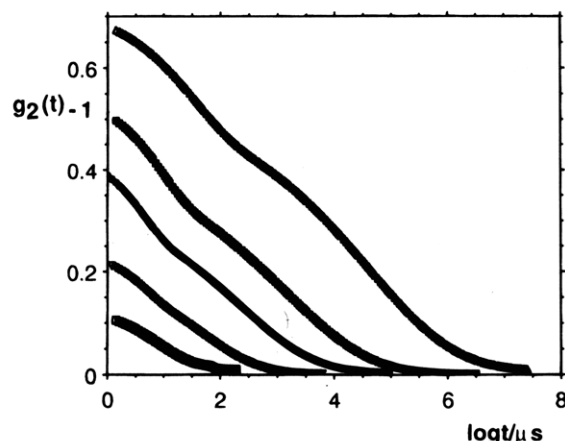


Figure 4. Measured orientation correlation functions for PnLMA at a scattering angle of 90° : (\square) $T = 293$, (∇) 276, (\bullet) 265, (\blacksquare) 253, and (\triangle) 244 K.

treated the DLS correlation functions in the homodyne limit. Under such conditions the measured intensity autocorrelation function $G_{V_H}(Q, t)$ is related to the desired normalized field correlation function $g_{V_H}(Q, t)$ (Q is the scattering vector with magnitude $(4\pi n/\lambda) \sin(\theta/2)$, with n being the refractive index, θ the scattering angle, and λ the laser wavelength) by

$$G_{V_H}(Q, t) = A[1 + f\alpha g_{V_H}(Q, t)]^2 \quad (1)$$

where f is the instrumental factor, calculated by means of a standard, α is the fraction of the total scattered intensity associated with fluctuations in the optical anisotropy with correlation times longer than 10^{-6} s and A is the baseline. Typical correlation functions obtained in the V_H geometry are shown in Figure 4 at temperatures in the range 244–293 K. The lower and upper temperature limits were determined by the crystallization and the width of the correlator window, respectively. The $g_{V_H}(Q, t)$ clearly displays two relaxation processes, and both can be well analyzed in the range 244–276 K. Correlation functions in the polarized (V_V) geometry were also measured and were influenced by the long-range density fluctuations known as “clusters”²⁶ and will not be discussed further here. Two types of analyses have been performed for the $g_{V_H}(t)$ correlation functions. First, we used a double Kohlrausch-Williams-Watts (KWW) function

$$\alpha g_{V_H}(Q, t) = \alpha_f \exp[-(t/\tau_f)^{\beta_f}] + \alpha_s \exp[-(t/\tau_s)^{\beta_s}] \quad (2)$$

with parameters $\alpha_{f,s}$, $\tau_{f,s}$, and $\beta_{f,s}$ which give the contrast, relaxation time, and shape of the fast and slow processes, respectively. From this type of analysis we found temperature-dependent parameters. The slow relaxation times, τ_s , had a stronger temperature dependence than the fast τ_f and both β_s and β_f increased with increasing temperature. To verify this finding, a second type of analysis which does not assume any functional form for the correlation functions was made with the use of the inverse Laplace transform (ILT) of the time-correlation functions (using CONTIN):²⁷

$$\alpha g_{V_H}(Q, t) = \int_0^\infty A(\tau) e^{-t/\tau} d\tau = \int_{-\infty}^{+\infty} \tau A(\tau) e^{-t/\tau} d(\ln \tau) \quad (3)$$

The results of the ILT analysis at different temperatures are illustrated in Figure 5. The ILT result shows a

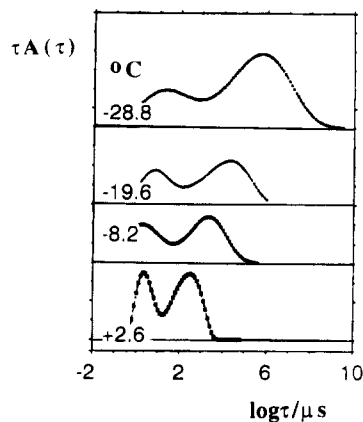


Figure 5. Retardation time spectra, $\tau A(\tau)$, at four temperatures as indicated obtained from the inversion of the time correlation functions using the ILT technique.

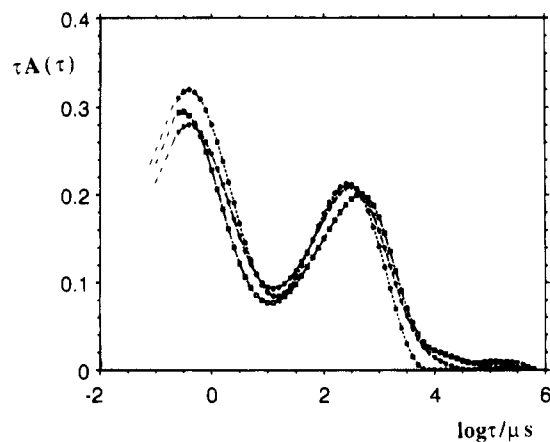


Figure 6. Inverse Laplace transformation of the V_H correlation functions at 276 K for three angles: (\circ) $\theta = 60^\circ$, (\square) $\theta = 90^\circ$, (\blacktriangledown) $\theta = 140^\circ$.

double peak structure with peaks which are broadened and shifted to longer times with decreasing temperature. The shift of the relaxation times is more prominent for the slower mode which additionally becomes narrower with increasing T . Figure 6 shows the result of the ILT for the data at 276 K at three angles. The absence of any detectable Q -dependence²⁸—for the light scattering Q 's (Figure 6)—and the stronger temperature dependence of the slower peak (Figure 5) are characteristic of density fluctuations above (α -relaxation) and below (β -relaxation) T_g . The fast relaxation process is assigned to the secondary (β -) relaxation mainly due to its weaker T -dependence as compared to the slow (α -) process. This β -process, however, should not be confused with the usual secondary relaxation in the lower members of poly(n -alkyl methacrylate) (see below). Last, the Q -independent α -process found by light scattering at low Q 's differs from the strong Q -dependence observed by neutron scattering at much higher Q 's.²⁹

Dielectric Spectroscopy (DS). Dielectric relaxation measurements of poly(n -alkyl methacrylates), including PnLMA, have been reported earlier.⁷ For PnLMA a single process (α -relaxation) was detected probably because of the smaller frequency range employed. In fact, we find three dielectrically active relaxations in the present study of PnLMA. Starting from high T , the first two processes correspond to the primary and secondary relaxations, also seen in DLS, and the third process is detected only at lower T (by DS). As with the DLS data, we have employed two types of analyses: The first assumes a specific shape

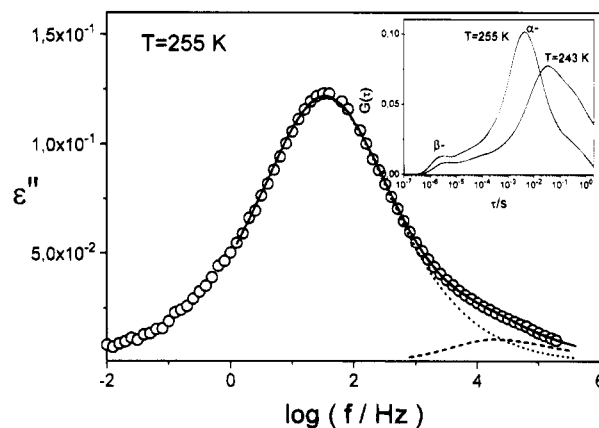


Figure 7. Fit of the dielectric loss data in PnLMA at $T = 255$ K using a double HN function. The “fast” and “slow” processes are the fast β - and α -relaxations, respectively. The distribution of relaxation times is shown in the inset at two temperatures.

given by the empirical equation of Havriliak and Negami (HN)³⁰

$$\epsilon^*(\omega) = \epsilon_\infty + \frac{\Delta\epsilon}{[1 + (i\omega\tau_{HN})^\alpha]^\gamma} \quad (4)$$

which has been very successful in describing the DS data from a variety of systems. In eq 4, $\Delta\epsilon$ is the relaxation strength of the process under investigation, τ_{HN} is the characteristic relaxation time of the HN equation, and α and γ respectively describe the symmetrical and asymmetrical broadening of the distribution of relaxation times. The electrical conductivity within the sample has also been fitted by $\epsilon''(\omega) \sim \omega^{-1}$. Figure 7 shows a fit with a double HN function to the dielectric loss data at $T = 255$ K. The second approach, which makes no assumption on the form of the relaxation function, is based on the inversion of the dielectric data

$$\frac{\epsilon''(\omega)}{\Delta\epsilon} = \int_{-\infty}^{+\infty} \tau A(\tau) \frac{\omega\tau}{1 + (\omega\tau)^2} d(\ln \tau) \quad (5)$$

again using CONTIN³¹ and provides directly the distribution of relaxation times $K(\tau) = \tau A(\tau) \Delta\epsilon$. The result from the inversion of the experimental data at $T = 255$ K is shown in the inset to Figure 7 and reveals a bimodal distribution. A single HN was used to fit the fastest process in the T -range: from 127 to 148 K. The dependence of the HN parameters on T for the three processes is discussed in the next section.

Mechanical Spectroscopy. From the dynamic mechanical measurements the master curves of G' and G'' are plotted in Figure 8 as a function of reduced frequency. Only horizontal shifts were applied to the data, and the reference temperature was $T_0 = 293$ K. The shift factors are also plotted in the inset to Figure 8. The WLF parameters at the reference temperature were $c_1^0 = 6.6$ and $c_2^0 = 118$ K which correspond to $c_1^g = 15$ and $c_2^g = 51$ K at T_g . The average relaxation time $\langle\tau\rangle$ was obtained from the isothermal data at $T = 238$ K which show the crossing of G' and G'' . The distribution of relaxation times was obtained by a Fourier transformation of the KWW function in the frequency domain and comparison with the G' and G'' data in the high-frequency portion of the softening region. Finally, from the values of $\langle\tau\rangle$ and β_{KWW} the τ_{max} was calculated.

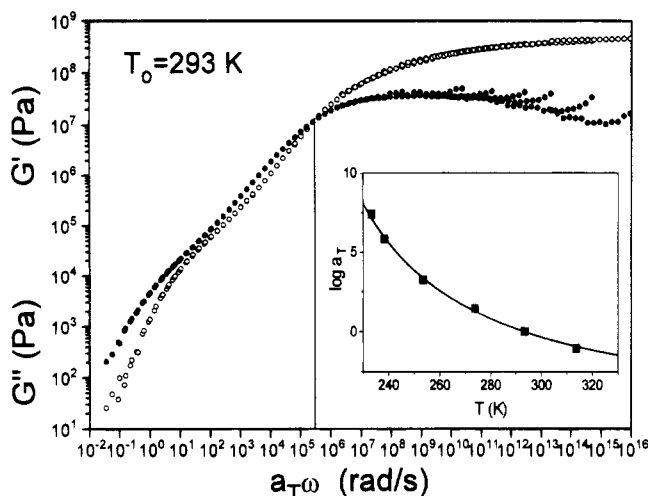


Figure 8. Reduced frequency plot for the G' and G'' of PnLMA using $T_0 = 293$ K as the reference temperature. The corresponding shift factors are plotted in the inset.

Results and Discussion

Rubbery State. The DS and DLS measurements give clear evidence for the existence of two processes at temperatures near and above the calorimetric T_g (Figures 4 and 7). Additionally, the MS measurements made over the high-frequency portion of the softening region are caused by the segmental relaxation (Figure 8), but the pronounced failure of the time-temperature superposition at lower T is indicative of another, faster relaxation with Arrhenius temperature dependence which is appropriate for a process below T_g . As mentioned in the preceding section, the slow and fast processes are identical with the primary (α -) and secondary (β -) relaxations, respectively. To facilitate the comparison of the distribution of relaxation times for the α -relaxation as obtained from DS and DLS, we have performed the Fourier transform of the dielectric complex permittivity $\epsilon^*(\omega)$ and fitted the resulting normalized autocorrelation function $\Phi(t)$ by the KWW function to obtain the exponent β_{KWW} . We are aware that in doing so we are only treating the width and not the exact shape of the dielectric loss data which are characterized by two shape parameters in the frequency domain, instead of the single shape parameter in the time domain. The T -dependence of the β_{KWW} as obtained from DS and DLS is shown in Figure 9 including the value of β_{KWW} from the dynamic mechanical data in the softening region. The distribution of relaxation times is very broad near T_g ($\beta_{\text{KWW}} \approx 0.25$) but narrows with increasing T , and at $T = 325$ K which is only 100 K above T_g the α -relaxation becomes practically a single exponential ($\beta_{\text{KWW}} \approx 1$). This point deserves more attention. It is usually the case with glass-forming liquids that the distribution of relaxation times narrows with T ,^{26,32} and at a high temperature which is near the melting temperature T_m and within the frequency range from gigahertz to terahertz the relaxation function approaches a single exponential (Debye process). Polymers behave differently^{32b,33,34} as follows: the distribution is quite broad near T_g , and this is reflected in the low values of β_{KWW} (in the range 0.3–0.4) or in the values of the HN parameters α and $\alpha\gamma$ and usually narrows with increasing T to a value which is smaller than one (usually $\beta_{\text{KWW}} \leq 0.5$). It has also been reported³⁵ that for some polymers the distribution of relaxation times (β_{KWW}) is insensitive to T . The unique feature of PnLMA so far is that it resembles a polymer-

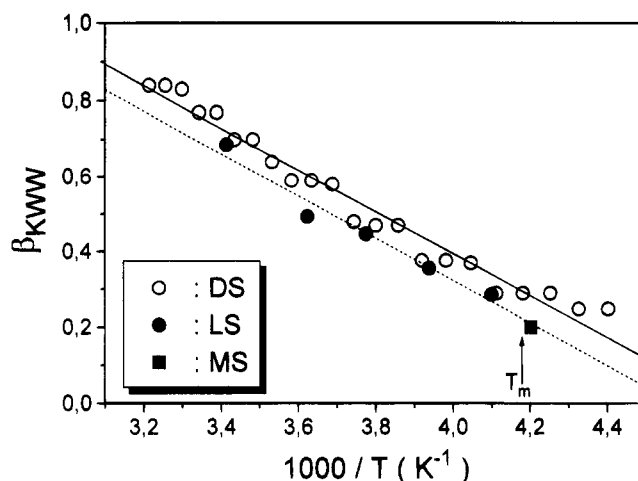


Figure 9. Kohlrausch-Williams-Watts exponent (β_{KWW}) of the segmental relaxation plotted vs inverse temperature. The melting point of PnLMA is indicated with an arrow.

like distribution of relaxation times near T_g ($\beta_{\text{KWW}} \approx 0.25$) and a small-molecule liquidlike distribution ($\beta_{\text{KWW}} \approx 0.9$) at higher T ($\approx T_g + 100$ K).

Alternatively, a low and strongly T -dependent β_{KWW} can also imply the existence of two processes with different T -dependences ($\alpha + \beta$ relaxation). We have investigated this issue in detail by making the inversion of the dielectric data using the modified version of CONTIN (eq 5). The distribution of relaxation times for the main peak in Figure 7 was found to broaden asymmetrically toward longer times with decreasing T . However, within the temperature range investigated it remained a single peak which suggests that the merging of the segmental (α -) with the slow β -relaxation occurred at times longer than about 10^2 s. Moreover, the well-known from other poly(*n*-alkyl methacrylates) slow β -relaxation would broaden the distribution (inset to Figure 7) toward short times. Therefore, the slow β -relaxation does not suffice to explain the asymmetric broadening of the distribution. Alternatively, such asymmetric broadening exists in polymer blends and copolymers (see below).

The distribution of relaxation times obtained from DS can be parametrized in the form

$$\beta_{\text{KWW}} = x - y/T \quad (6)$$

with parameters (x, y) equal to (2.615, 555), whereas from DLS these parameters are (2.573, 562). The single β_{KWW} value obtained from the MS measurements agrees with the extrapolation by eq 6 from the DLS data. However, given the uncertainty in the estimation of β_{KWW} by different methods, we conclude that DS and DLS are practically sensitive to the same distribution of relaxation times for the segmental (α -) relaxation originating from the dipole moment and optical anisotropy, respectively, of the COOR group which is attached to the main chain. The linear dependence of β_{KWW} with inverse temperature may reflect a relation between fragility and topology.³⁶ The majority of "strong" liquids have a well-defined network glass structure with a low value of the average coordination number z_0 (typically $z_0 \approx 3-5$) and of its fluctuations (Δz), whereas "fragile" liquids have higher coordination numbers (typically $z_0 \approx 14-16$) and higher fluctuations Δz . The two parameters above (z and Δz) suffice to explain³⁷ the strong vs fragile behavior of liquids, whereas the distribution of relaxation times is only affected by the latter, i.e., β_{KWW}

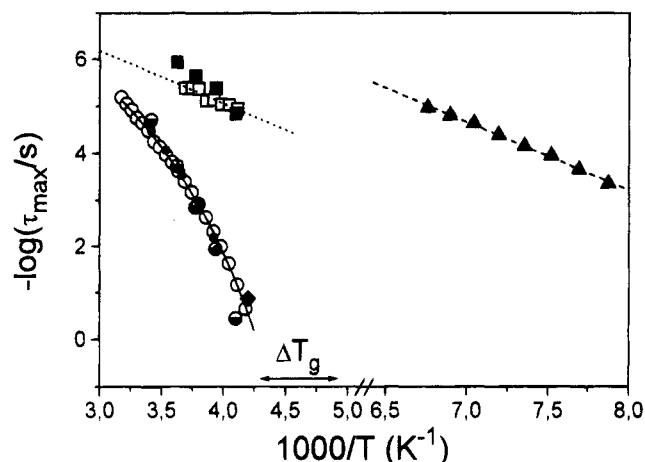


Figure 10. Temperature dependence of the relaxation times of PnLMA in an Arrhenius representation. The α -relaxation times are from (○) DS (present study), (●) DS from ref 7, (●) DLS, and (◆) MS. The β -relaxation times are from (□) DS and (■) DLS. The low- T relaxation (γ -process (▲)) times are obtained from DS.

$\approx 1 - \Delta z E_0/T$ where E_0 is the variance in the energy of the system. According to this recently published model,³⁷ the temperature dependence of β_{KWW} (eq 6) can be attributed to the reduction in the fluctuations of the coordination number Δz ($\Delta z \rightarrow 0$) with increasing T . This implies a structural change with T .

In Figure 10, we plot the T -dependence of the relaxation times for the α -relaxation and the lower T relaxations (β - and γ -) as probed by DS. Previous DS measurements⁷ on the segmental relaxation lie practically on top of our relaxation times. The DLS relaxation times are also plotted in Figure 10 and compare well with the times obtained from DS. We have to mention that differences between DLS and DS with respect to the different order of the Legendre polynomials of the orientational correlation functions are suppressed in the logarithmic scale of Figure 10. The broad ΔT_g , as obtained from DSC, is also indicated in Figure 10. The Vogel–Fulcher–Tammann (VFT) equation

$$\tau = \tau_0 \exp[B/(T - T_0)] \quad (7)$$

was used to fit the segmental relaxation times with three parameters, τ_0 , B , and T_0 , which represent the high- T intercept, the apparent activation energy, and the “ideal” glass transition temperature T_0 , being lower than the calorimetric T_g ($T_0 = T_g - c_2^g$). The VFT fit to the DS data yields $\tau_0 = 8.7 \times 10^{-10}$ s, $B = 1300 \pm 100$ K, and $T_0 = 172 \pm 2$ K. Notwithstanding the similarity of the T_0 value with the one from MS, the high-temperature intercept of the VFT fit to the data shown in Figure 10, is about 4 decades slower than the generally accepted value ($\approx 10^{-14}$ s). On the other hand, a forced fit (with $\tau_0 = 10^{-14}$ s) results in $T_0 = 110$ K. A recent³⁸ study of the dynamics of some glass-forming liquids which involved the analysis of the temperature derivatives of the dielectric relaxation times has shown that a single VFT fails even for temperatures near T_g . For the glass-forming liquid salol, a fit to the VFT was only possible at $T > T_g + 45$ K, resulting, however, in a low value for the high- T intercept.

An alternative approach³⁹ has been proposed for the analysis of viscosity $\eta(T)$ and relaxation times $\tau(T)$ for the α -process of supercooled liquids. It has been argued that $\eta(T)$ and $\tau(T)$ from fragile and strong liquids can be scaled on a single universal curve, at $T > T_g$, using

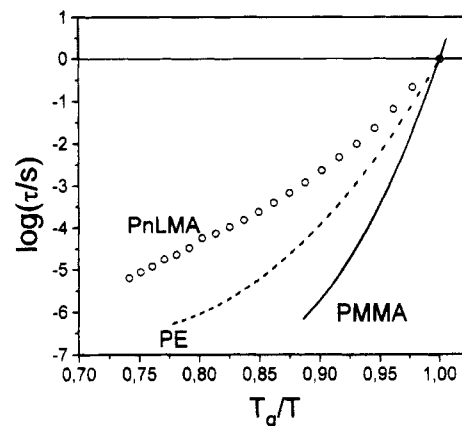


Figure 11. T_g -scaled temperature dependence of the segmental relaxation times of PnLMA (○), in comparison with PMMA¹⁶ and PE³⁵. The glass transition temperature T_g is defined as the temperature at which the relaxation time is 1 s.

species-dependent adjustable parameters. The scaling temperature (T^* in this model) is located above the melting point T_m and signifies the temperature below which collective motions begin to play a role. On the basis of this analysis, we find a T^* ($=291$ K) for PnLMA which is well above T_m and a small degree of clustering typical of strong liquids.

To estimate the degree of cooperativity^{17–19} or “fragility”³⁶ of PnLMA and to compare that with other polymers, we plot in Figure 11 the relaxation times for the segmental relaxation vs the T_g -scaled temperature (T_g/T). To avoid the complication from the very broad transition range and unnecessary extrapolations, we define an operational T_g as the temperature at which $\tau = 1$ s. This kind of representation of the segmental relaxation times was shown to be very useful in comparing different systems.¹⁷ It has also been called the “cooperativity” plot since the curvature at $T \approx T_g$ was found to increase in the same order as the value of $n^* = 1 - \beta_{KWW}$. The latter (n^*) reflects the capacity of intermolecular coupling which assumes different values depending on the chemical structure of the system. A compilation⁴⁰ of segmental relaxation times from n -alkyl methacrylates has shown that the degree of curvature or steepness index $m = d \log \tau / d(T_g/T)$, evaluated at $T \approx T_g$, decreases monotonically with increasing length of the side chain. In Figure 11 we include the relaxation times of PMMA¹⁶ and polyethylene (PE),¹⁸ keeping the same definition of T_g (as $\log \tau = 0$). Figure 11 shows that PnLMA is a very strong glass, stronger than PE, and the values of m at T_g are 30, 45, and 66 for PnLMA, PE, and PMMA, respectively.

A comparison of existing relaxation data¹⁹ from a large number of polymers, ionic melts, supercooled liquids, and covalent glass formers has shown that the correlation of the nonexponentiality of the α -relaxation with the cooperativity can be parametrized as $m = 250 (\pm 30) - 320\beta_{KWW}$, where β_{KWW} refers to its value of T_g . Given the low value of m for PnLMA and using the empirical relation above, we obtain a value of 0.7 ± 0.1 for β_{KWW} at T_g , which is much larger than the measured value (≈ 0.25). This deviation, however, is apparent, and the low β_{KWW} value reflects a heterogeneous broadening related to the nature of the polymer. PnLMA has long polyethylene-like side chains which blend with the parts of the monomer units near the main chain (i.e., the methacrylate backbone). There is a preponderance of methylene molecules in the vicinity of the methacrylate

backbone, which reduces the probability of finding other methacrylate backbone molecules in its vicinity. As a result, intermolecular cooperativity in the motion of the methacrylate backbone molecule involves to a great extent the surrounding methylene molecules in the side chains. Among entirely carbon backbone polymers, the methylene chains having the simplest chemical structure possible are most flexible and impose the least dynamic constraints on each other or on another kind of molecule like the methacrylate backbone. There is, therefore, a mitigation of the intermolecular (and even possibly the intramolecular) dynamic constraints between the methacrylate backbone molecules by the intervening methylene chains. In the framework of the coupling model this mitigation of dynamic constraints will result in a decrease of the coupling parameter n^* ($=1 - \beta$) of the segmental motion and consequently¹⁷⁻¹⁹ a smaller steepness index m in PnLMA when compared with PMMA ($R = CH_3$). In fact, segmental motion in PnLMA should have a low degree of cooperativity and small n^* and m as in PE. A complication, however, arises from the fact that PE is a semicrystalline material and this can artificially broaden the segmental relaxation of the amorphous phase. When the PE-like side chain is attached to the PMMA-like backbone, concentration fluctuations are created in a somewhat similar fashion to miscible binary polymer blends or block copolymers, with the backbone and side chain playing the roles of the two polymers. Theoretical models⁴¹ based on concentration fluctuations were successful in describing quantitatively the broadening of the segmental relaxation in homogeneous amorphous polymer blends.⁴² The existence of concentration fluctuations in poly(*n*-alkyl methacrylates) has been reported by combined SAXS and pressure-volume-temperature (PVT) measurements for the lower members of the series ($n \leq 6$).⁴³ It has been shown that the measured total fluctuations by SAXS exceed the calculated density fluctuations from the measured isothermal compressibility and this difference was found to depend on the length of the side chain. The extremely broad segmental relaxation of PnLMA at $T \approx T_g$ reflects the heterogeneous broadening by the presence of concentration fluctuations of backbone and side-chain units. As seen before in miscible binary blends^{41,42} at high T , however, the broadening due to concentration fluctuations diminishes and the distribution now reflects intermolecular cooperativity like the situation in one-component systems. Nevertheless, $\beta_{KWW} \approx 1$ at high T for a polymeric melt can be hardly explained by such models and might reflect the dynamic dominance of the long and flexible side group.

Glassy State. The secondary process (β -relaxation) of poly(*n*-alkyl methacrylates) has been studied mainly by DS. It was found that the increase in the length of the alkyl side chain made the separation between the α - and β -processes increasingly more difficult to detect⁴⁻⁷ just as in dynamic mechanical measurements.³ Pressure was subsequently applied to separate the two processes, and it was found to be very successful for the lower poly(*n*-alkyl methacrylates).^{5,7} However, the earlier⁷ and the present DS studies have shown no evidence of the expected β -relaxation. The reason for the absence of the well-known β -relaxation from the DS spectra of PnLMA lies in the systematic shift of the splitting zone between the α - and β -relaxations to lower frequencies. The shift is predicted⁴⁴ to be about 2 decades per CH_2 -unit in the alkyl chain and therefore becomes too slow

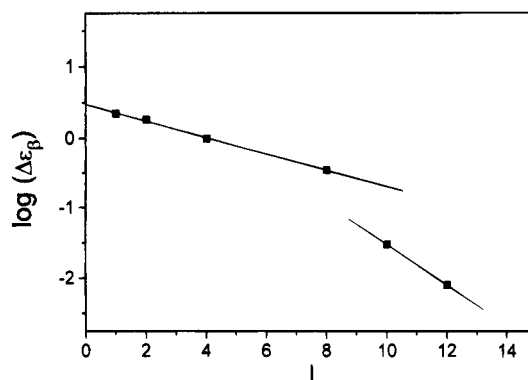


Figure 12. Dependence of the dielectric strength, $\Delta\epsilon$, for the β -process at $T \approx T_g$ on the number of carbon atoms on the side chain in poly(*n*-alkyl methacrylates). The data for $l \leq 8$ are from ref 5.

to be detected. The inversion of the experimental data at low T (Figure 7) gave, again, no evidence for a splitting between the α -relaxation and slow β -relaxation. Here we are able to resolve a new and faster relaxation (which we call fast β -relaxation) using a broader frequency range. As we discuss below, the main difficulty in observing this new relaxation lies in its small dielectric strength. In Figure 12, we compare the dielectric strength of the slow β -relaxation in different poly(*n*-alkyl methacrylates) with the faster β -relaxation in PnLMA and poly(*n*-decyl methacrylate) (PnDMA)⁴⁵ as a function of the carbon atoms in the alkyl chain. The strength $\Delta\epsilon_\beta$ in Figure 12 refers to its value at T_g . It can be seen that the fast β -process detected for $l \geq 10$ has a different origin from the slow β -relaxation found in $l \leq 8$. The decrease $\Delta\epsilon_\beta$ in the latter case has been interpreted as a dilution effect of the dipole density per unit volume with increasing l .

The distribution of the DS relaxation times of the fast β -process can be parametrized by the HN parameters (eq 4) $\alpha = 0.8$ and $\gamma = 0.4$, resulting in a β_{KWW} of ~ 0.4 . Using this value as a fixed parameter, we obtained unique fits using the KWW function (eq 2) to the DLS data. Alternatively, the procedure described in the data analysis was used to invert both the DLS (eq 3) and DS (eq 5) spectra using CONTIN, and this procedure gave consistent results. The relaxation times for the fast β -relaxation, plotted in Figure 10, are fitted with an Arrhenius law ($T_0 = 0$ K in eq 6), with intercept $\tau_0 = 3.2 \times 10^{-10}$ s and activation energy $E = 5.1$ kcal/mol. The DLS relaxation times (also plotted in Figure 10) give $\tau_0 = 10^{-14}$ s and $E = 10$ kcal/mol, and the differences in the activation parameters are due to the limited T -range for which the β -relaxation can be investigated. Both activation energies are much smaller than for the slow β -relaxation in poly(*n*-alkyl methacrylates). For the latter process it was found that an increase in the length of the side chain results in an increase of the activation energy.⁵ For example, the activation energies are 21, 24, and 28 kcal/mol for PMMA, PEMA, and PnBMA, respectively, as a result of the hindrance to the side-chain motion. The lower activation energy for the fast β -relaxation of PnLMA reflects a more localized motion. It is interesting to note that the activation energy of this process is similar to that for the mechanical γ -relaxation in PE ($E_\gamma \approx 11$ kcal/mol) which appears at $T = 126$ K for $f = 1$ Hz.⁴⁶ We can, therefore, assign this process to a localized hindered rotation of the side chain.

At lower T another relaxation exists (γ -relaxation) in the DS experiment of a very small relaxation strength

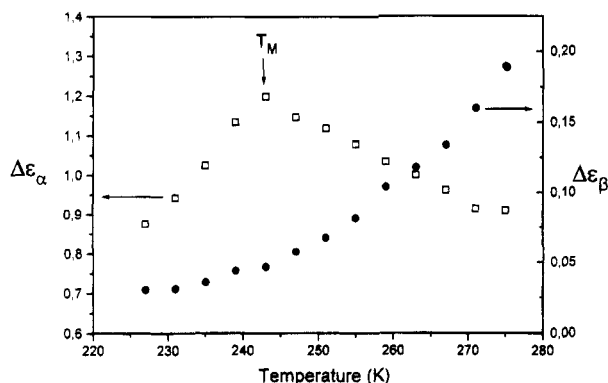


Figure 13. Temperature dependence of the relaxation strength for the α - (\square) and β -processes (\bullet) in PnLMA. The vertical arrow indicates the melting temperature.

($\Delta\epsilon = 2 \times 10^{-2}$). It has the following activation parameters: $\tau_0 = 1.6 \times 10^{-15}$ s and $E_\gamma = 6.6$ kcal/mol. This process may correspond to the mechanical γ -relaxation found in poly(*n*-alkyl methacrylates) with $l \geq 3$ and with an activation energy $E_\gamma \approx 5.5$ kcal/mol ($T_{\max} = 90$ K at $f = 0.5$ Hz). This process has been assigned to the rotation of the ethyl end group.³

The temperature dependencies of the dielectric strength of the α - and β -processes are shown in Figure 13. The dielectric strength of the α -relaxation ($\Delta\epsilon_\alpha$) increases with increasing T and shows a maximum in the vicinity of the melting point (arrow in Figure 13). For temperatures below T_m the hindered mobility of the side-chain motion results in the decrease of $\Delta\epsilon_\alpha$. The temperature dependence of $\Delta\epsilon_\beta$ is opposite. $\Delta\epsilon_\beta$ increases with increasing T as a result of the increase in the number of dipoles participating in the motion. Notice the smaller values of $\Delta\epsilon_\beta$ as compared to $\Delta\epsilon_\alpha$ at all T .

Conclusion

The study of the dynamics of PnLMA revealed some interesting features which are not common to the lower members of the series of poly(*n*-alkyl methacrylates). In PnLMA, the splitting of the segmental (α -) from the slow β -relaxation occurs at low frequencies, and we can practically study the mixed ($\alpha\beta$ -) relaxation over a broad temperature range. On the basis of the T -dependence of the relaxation times, we find that the mixed ($\alpha\beta$ -) relaxation has the character of an α -relaxation (non-Arrhenius) with a peculiar variation of the distribution function with T . The distribution of relaxation times,⁴⁷ obtained from the combined DLS and DS experiments, is exceptionally broad near T_g , but it displays a strong T -dependence and at a frequency of 1 MHz collapses into a Debye process. Consequently, PnLMA is, to our knowledge, the only polymer with nearly a Debye segmental relaxation at megahertz frequencies. The characteristic relaxation time when plotted against normalized reciprocal temperature, T_g/T , shows a very weak dependence. The strong nature of this glass cannot simultaneously account for the narrow distribution of relaxation times at high T and the very broad distribution near T_g . The latter can be explained if we envision PnLMA as a copolymer made out of a PMMA-like backbone with a PE-like side chain. Then the temperature-dependent broadening of the segmental relaxation can be attributed to the concentration fluctuations from the methacrylate backbone and side-chain molecules. The actual contribution of intermolecular cooperativity to the breadth of the segmental relaxation

in PnLMA is quite small. This follows in the coupling model from the small coupling parameter n due to the much reduced intermolecular dynamic constraints, compared with the situation in PMMA, caused by the preponderance of methylene chain molecules near the methacrylate backbone in PnLMA. A small n^* also gives rise in the coupling model to a weak dependence of T_g/T . Thus, the rather unique features of the segmental relaxation dynamics observed experimentally in this work can be explained. At lower temperatures, additional relaxation processes exist of more local nature which are associated with the alkyl side chain.

Acknowledgment. We thank D. J. Plazek and T. Pakula for reading the paper. W.B. and P.S. acknowledge the support of the Swedish Natural Science Research Council NFR. K.L.N. is supported in part by ONR Contract N0001495WX20203. P.S. acknowledges the support of the Grant Agency of the Czech Republic through Grant No. 203/94/0817. Partial support to FORTH and Max-Planck-Institut from the EC HCM-Network project (CT920009) is gratefully acknowledged.

References and Notes

- (1) For a review, see: McCrum, N. G.; Read, B. E.; Williams, G. *Anelastic and Dielectric Effects in Polymeric Solids*; Dover, Inc.: New York, 1991.
- (2) For references, see: Ferry, J. D. *Viscoelastic Properties of Polymers*, 3rd ed.; Wiley and Sons: New York, 1980.
- (3) Heijboer, J.; Pineri, M. In *Nonmetallic Materials and Composites at Low Temperatures*; Hartwig, G., Evens, D., Eds.; Plenum Publ. Co.: New York, 1982; Vol. 2, and ref 1, p 244.
- (4) Ishida, Y.; Yamafuji, K. *Kolloid Z.* **1961**, 177, 97.
- (5) Sasabe, H.; Saito, S. *J. Polym. Sci.* **1968**, A2-6, 1401.
- (6) Meier, G.; Kremer, F.; Fytas, G.; Rizos, A., preprint.
- (7) Williams, G.; Watts, D. C. *Trans. Faraday Soc.* **1971**, 67, 2793.
- (8) Fytas, G.; Wang, C. H.; Fischer, E. W.; Mehler, K. *J. Polym. Sci., Polym. Phys. Ed.* **1986**, 24, 1854; *Macromolecules* **1988**, 21, 2253.
- (9) Patterson, G. D.; Stevens, J. R.; Lindsey, C. P. *J. Macromol. Sci.* **1981**, B18, 641.
- (10) Meier, G.; Fytas, G.; Dorfmueller, Th. *Macromolecules* **1984**, 17, 957.
- (11) Patterson, G. D.; Jue, P. K.; Stevens, J. R. *J. Polym. Sci.* **1990**, B28, 481.
- (12) Giebel, L.; Meier, G.; Fytas, G.; Fischer, E. W. *J. Polym. Sci., Polym. Phys. Ed.* **1992**, 30, 1291.
- (13) Fytas, G. *Macromolecules* **1989**, 22, 211.
- (14) Ribes-Greus, A.; Gomez-Ribelles, J. L.; Diaz-Calleja, R. *Polymer* **1985**, 26, 1849.
- (15) Floudas, G.; Fytas, G.; Fischer, E. W. *Macromolecules* **1991**, 24, 1955.
- (16) Floudas, G.; Rizos, A.; Brown, W.; Ngai, K. L. *Macromolecules* **1994**, 27, 2719.
- (17) Ngai, K. L. *J. Non-Cryst. Solids* **1987**, 98-99, 969. Plazek, D. J.; Ngai, K. L. *Macromolecules* **1991**, 24, 1222.
- (18) Ngai, K. L.; Roland, C. M. *Macromolecules* **1993**, 26, 6824.
- (19) Bohmer, R.; Ngai, K. L.; Angell, C. A.; Plazek, D. J. *J. Chem. Phys.* **1993**, 99, 4201.
- (20) Rogers, S. R.; Mandelkern, L. *J. Phys. Chem.* **1957**, 61, 985.
- (21) Greenberg, S. A.; Alfrey, T. J. *J. Phys. Chem.* **1954**, 76, 6280.
- (22) Plate, N. A.; Shibaev, V. P.; Petrukhin, B. S.; Kargin, V. A. *J. Polym. Sci.* **1968**, C-23, 37.
- (23) Floudas, G.; Pakula, T.; Stamm, M.; Fischer, E. W. *Macromolecules* **1993**, 26, 1671.
- (24) Miller, R. L.; Boyer, R. F.; Heijboer, J. *J. Polym. Sci., Polym. Phys. Ed.* **1984**, 22, 2021.
- (25) Kremer, F.; Boese, D.; Meier, G.; Fischer, E. W. *Progr. Colloid Polym. Sci.* **1989**, 80, 129.
- (26) Fischer, E. W. *Physica* **1993**, A201, 183.
- (27) Provencher, S. W. *Comput. Phys. Commun.* **1982**, 27, 229.
- (28) Wang, C. H.; Fytas, G.; Lilje, D.; Dorfmueller, Th. *Macromolecules* **1981**, 14, 1363. Fytas, G.; Floudas, G.; Ngai, K. L. *Macromolecules* **1990**, 23, 1104.
- (29) Ngai, K. L.; Colmenero, J.; Alegria, A.; Arbe, A. *Macromolecules* **1992**, 25, 6727. Floudas, G.; Higgins, J. S.; Fytas, G. *J. Chem. Phys.* **1992**, 96, 7672. Zorn, R.; Richter, D.; Farago,

- B.; Frick, B.; Kremer, F.; Kirst, U.; Fetters, L. J. *Physica B* **1992**, 180-181, 534. Colmenero, J.; Alegria, A.; Arbe, A.; Frick, B. *Phys. Rev. Lett.* **1992**, 69, 478.
- (30) Harviliak, S.; Negami, S. *Polymer* **1967**, 8, 161.
- (31) Alvarez, F. Ph.D. Thesis, Universidad del Pais Vasco, Spain, 1993. Karatasos, K.; Anastasiadis, S. H.; Semenov, A. N.; Fytas, G.; Pitsikalis, M.; Hadjichristidis, N. *Macromolecules* **1994**, 27, 3543.
- (32) (a) Dixon, P. K.; Nagel, S. R. *Phys. Rev. Lett.* **1988**, 61, 341. (b) Schönhals, A.; Kremer, F.; Schlosser, E. *Phys. Rev. Lett.* **1991**, 67, 999. (c) Dixon, P. K.; Wu, L.; Nagel, S. R.; Williams, B. D.; Carini, J. P. *Phys. Rev. Lett.* **1990**, 65, 1108.
- (33) (a) Floudas, G.; Higgins, J. S.; Kremer, F.; Fischer, E. W. *Macromolecules* **1992**, 25, 4955. (b) Schönhals, A.; Schlosser, E. *Colloid Polym. Sci.* **1989**, 267, 125; **1989**, 267, 133.
- (34) Matsuoka, S.; Quan, X. *Macromolecules* **1991**, 24, 2770.
- (35) Boese, D.; Kremer, F. *Macromolecules* **1990**, 23, 829. Alvarez, F.; Colmenero, J.; Kanetakis, J.; Fytas, G. *Phys. Rev. B* **1994**, 49, 14996.
- (36) Angell, C. A. *J. Non-Cryst. Solids* **1991**, 131-133, 13. Angell, C. A. In *Relaxation in Complex Systems*; Ngai, K. L., Wright, G. B., Eds.; Naval Research Laboratory: Washington, DC, 1985.
- (37) Vilgis, T. A. *Phys. Rev. B* **1993**, 47, 2882; *J. Phys.: Condens. Matter* **1990**, 2, 3667.
- (38) Stickel, F.; Fischer, E. W.; Richter, R. *J. Chem. Phys.* **1995**, 102, 6251.
- (39) Kivelson, S. A.; Zhao, X.; Fischer, T. M.; Knobler, C. M. *J. Chem. Phys.* **1994**, 101, 2391.
- (40) Ngai, K. L.; Plazek, D. J. *Handbook of Polymer Properties*; American Institute of Physics: 1995.
- (41) Zetsche, A.; Fischer, E. W. *Acta Polym.* **1994**, 45, 168. Roland, C. M.; Ngai, K. L. *Macromolecules* **1991**, 25, 363. Alegria, A.; Colmenero, J.; Ngai, K. L.; Roland, C. M. *Macromolecules* **1994**, 27, 4486.
- (42) Zetsche, A.; Kremer, F.; Jung, W.; Schulze, H. *Polymer* **1990**, 31, 1883. Chung, G.-C.; Kornfield, J. A.; Smith, S. D. *Macromolecules* **1994**, 27, 5729; **1994**, 27, 964.
- (43) Floudas, G.; Pakula, T.; Fischer, E. W. *Macromolecules* **1994**, 27, 917.
- (44) Beiner, M.; Garwe, F.; Schroter, K.; Donth, E. *Colloid Polym. Sci.* **1994**, 272, 1439. Garwe, F.; Beiner, M.; Hempel, E.; Schawe, J.; Schroter, K.; Schönhals, A.; Donth, E. *J. Non-Cryst. Solids* **1994**, 172-174, 191.
- (45) Placke, P., unpublished data.
- (46) Pineri, M.; Berticat, P.; Marchal, E. *J. Polym. Sci., Polym. Phys. Ed.* **1976**, 14, 1325.
- (47) A recent study [Böhmer, R.; Schiener, B.; Hamberger, J.; Chamberlin, R. V.] of PnLMA using a pulsed dielectric technique revealed a broad distribution of relaxation times at $T = 245$ K, in agreement with the dielectric data presented here.

MA950480S